

Magnetic Ordering in RbNiCl_3 †

W. B. Yelon and D. E. Cox

Brookhaven National Laboratory, Upton, New York 11973

(Received 4 February 1972)

The magnetic structure of RbNiCl_3 has been carefully reexamined by single-crystal neutron-diffraction techniques in light of a discrepancy between two previously reported powder neutron-diffraction results. Data were taken on a small single crystal at 4.5°K and were corrected for absorption and extinction. The results confirm the basic picture of a multidomain triangular arrangement with the moments lying in a plane perpendicular to the basal plane of the hexagonal crystal. However, a slight modification of this structure consistent with the symmetry and the presence of a small c -axis anisotropy yields a significantly better fit to the data. The magnetization was measured from 4.5 to 11.1°K [$T_N = (11.15 \pm 0.05)$ °K], and an attempt was made to determine the exponent β . The best fit to a simple power law gives $2\beta = 0.50 \pm 0.03$. However, a reasonable correction to the power law yields $2\beta = 0.60 \pm 0.03$. The Ni^{2+} moment extrapolated to 0°K is $(1.3 \pm 0.1)\mu_B$, indicative of very substantial zero-point effects.

I. INTRODUCTION

RbNiCl_3 is one of a group of isostructural compounds which have recently been the subject of considerable study. In these compounds there are chains of octahedrally coordinated $3d$ -transition-metal ions along the c axis. These chains are separated in the basal plane by about 7 Å and consequently the compounds show magnetic behavior which is predominantly one dimensional.^{1,2}

RbNiCl_3 orders antiferromagnetically at about 11°K. Two quite different magnetic structures have been reported on the basis of powder-neutron-diffraction data. Minkiewicz *et al.*³ reported a structure in which the antiferromagnetic chains of moments were coupled in a triangular array, while, according to Epstein *et al.*,⁴ the chains form a collinear structure with the moments directed along the c axis. The latter structure gives rise to an additional set of very weak powder diffraction peaks and, in order to investigate this point more carefully, we have obtained data from single crystals of RbNiCl_3 . The results are accounted for satisfactorily on the basis of the triangular model, with the spin plane perpendicular to the basal plane, although a slight modification of that triangular arrangement gives significantly better agreement. In contrast, the collinear model gives quite unacceptable agreement.

The value of the Ni^{2+} moment derived from the modified triangular model extrapolated to 0°K is found to be $1.3\mu_B$, much less than the value of $2\mu_B$ usually found for Ni^{2+} in approximately octahedral coordination. These findings closely parallel those of a recent investigation⁵ (referred to as Paper I) on a single crystal of CsNiCl_3 .

II. STRUCTURE REFINEMENT

The RbNiCl_3 crystals were grown from a melt

by the Bridgman technique.⁶ Chemical analysis gave the following composition (wt %) with the theoretical proportions in parentheses: Rb 34.5 (34.1), Ni: 23.4 (23.4), and Cl: 42.4 (42.5). A relatively small crystal, measuring only $0.3 \times 0.35 \times 0.25$ cm, was selected for study in order to minimize extinction effects. Data were obtained from the (hhl) zone at 4.5°K with neutrons of 1.20-Å wavelength. The data were corrected for extinction and absorption in exactly the same manner as in the previous study⁵ of CsNiCl_3 . Equivalent reflections of the type (hhl) and ($hh\bar{l}$) were measured and found to agree within 5% for the nuclear peaks and to within 5–10% for the magnetic peaks.

The magnetic reflections were found to appear at positions $(\frac{1}{3}h, \frac{1}{3}h, l)$ with $h \neq 3n$ and $l = 2n + 1$, which is characteristic of a tripled magnetic cell. There was very little intensity at the (111) position, and no significant changes were observed when the crystal was heated above the transition temperature. Even in the unlikely event that this was magnetic in origin and not due to multiple reflection, the collinear structure can be ruled out at once as this would require considerable scattering at this position, more than ten times greater than was actually observed. The results of a nuclear-structure least-squares refinement are listed in Table I. In Table II the observed and calculated nuclear intensities (corrected for absorption) are

TABLE I. Parameter values obtained from a least-squares refinement of the nuclear intensity data from RbNiCl_3 at 4.5°K.

Cl(x)	0.159(8)	± 0.001
β over all (Å ²)	0.37	± 0.06
Extinction coefficient	570	± 70
Scale factor	103.3	± 3.1

TABLE II. Comparison of observed and calculated nuclear intensities for RbNiCl_3 . I_{obs} is the observed intensity corrected for absorption. I_{calc} is the calculated intensity based upon the parameters in Table I. Scattering lengths taken as 0.705×10^{-12} , 1.03×10^{-12} , and 0.963×10^{-12} cm for Rb, Ni, and Cl, respectively.

hkl	$I_{\text{obs}} (\times 10^{-3})$	$I_{\text{calc}} (\times 10^{-3})$
110	5.9	6.4
220	76.6	73.1
330	3.0	3.0
440	41.4	43.7
002	45.5	46.5
112	10.6	10.5
222	24.0	25.0
332	4.4	4.3
004	71.5	68.4
114	2.7	2.6
224	56.4	54.6
334	2.5	2.5
006	18.8	18.8
116	5.2	4.8
226	15.6	16.5

compared.

Attempts were made to fit the magnetic data to a number of models consistent with the tripled magnetic unit cell and the absence of the (111) reflection. Some of these models (Fig. 1) are the same as those considered in Paper I, and, as before, satisfactory fits are obtained both for model IIa, a triangular spin arrangement in which the spin plane is perpendicular to the basal plane and in which there are equal fractions of equivalent magnetic domains, and model IIb, a single-domain triangular spin arrangement in which the spin plane is perpendicular to the basal plane and makes an angle of $\theta = 32^\circ$ to the [110] direction. The latter gives a better fit to the data, but it should be noted that for $\theta = 45^\circ$ the two models have identical structure-factor expressions. Since this ambiguity had also arisen in the CsNiCl_3 work, a second much larger crystal was oriented so as to

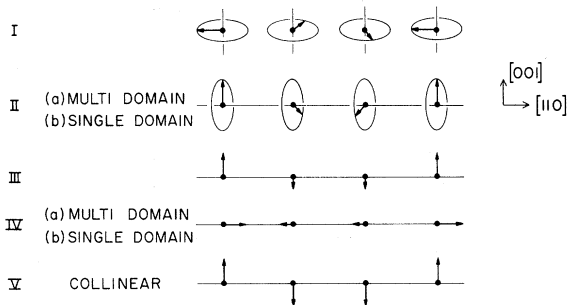


FIG. 1. Models I-V for the magnetic structure of RbNiCl_3 consistent with the observed magnetic unit cell. These models are completely described in Paper I.

give pairs of equivalent reflections of the type $(\frac{1}{3}h, \frac{1}{3}k, l)$ and $(\frac{1}{3}(-h-k), \frac{1}{3}k, l)$, which should have equal intensities in the multidomain structure but in general unequal values for the case of a single domain. These reflections were in fact found to have equal intensities to within the error limits of 5–10% observed for equivalent magnetic peaks in the (hhl) zone. The multidomain model is therefore strongly favored.

A triangular arrangement in which all the moments are equal and at precisely 120° to each other minimizes the exchange energy of a hexagonal network of moments in which there are only negative nearest-neighbor basal-plane interactions, but has trigonal symmetry only if the moments lie in the basal plane. An ac orientation implies the existence of a competing uniaxial anisotropy, and in this case the trigonal symmetry is lost and modifications of the triangular structure become possible.

We have therefore extended the data analysis to include model VI (Fig. 2), a generalized model with orthorhombic symmetry in which the moment (μ_1) on site A is directed along the c axis and the two site-B moments (μ_2) are canted at an angle of $\pm\theta$ to the c axis (Fig. 3). The triangular arrangement is simply the special case for which $\mu_1 = \mu_2$ and $\theta = 60^\circ$.

Surprisingly, a multidomain model of this type with $\theta = 57.5^\circ$ and $\mu_1 \approx \mu_2 = 1.25\mu_B$ gives precisely the same fit to the data as the single-domain triangular model IIb. Although the model can be described in terms of the tripled hexagonal cell ($a\sqrt{3}, a\sqrt{3}, c$) shown in Fig. 3, the magnetic symmetry is in fact orthorhombic with a C -centered cell having dimensions $3a, a\sqrt{3}, c$. The highest-symmetry magnetic space group consistent with model VI is $Cm'c2'_1$, which requires that the component of the moments in the basal plane lie parallel to the x axis in each of the three equivalent orthorhombic domains.

There is yet a further possible structure (model

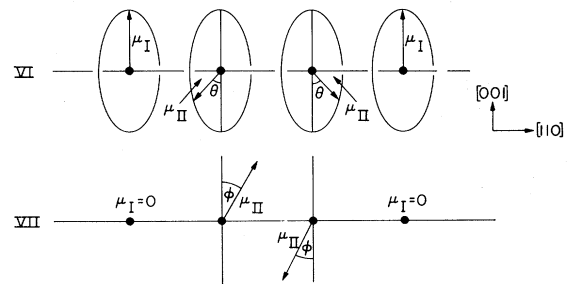


FIG. 2. Two additional models for the structure of RbNiCl_3 , to which the data were fitted. The symmetry of model VI is orthorhombic, while that of model VII is monoclinic.

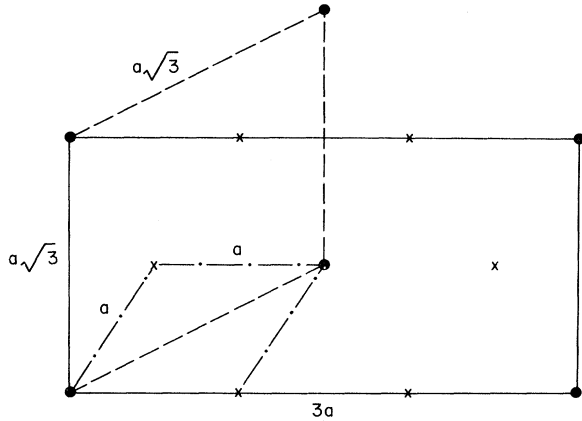


FIG. 3. Basal-plane projection of the unit cells of RbNiCl_3 . The dot-dash lines correspond to the chemical unit cell with dimensions a , a , c . The enlarged cell (dashed lines) with dimensions $a\sqrt{3}$, $a\sqrt{3}$, c is the smallest cell consistent with the observed magnetic peaks (the unit cell for neutron scattering), while the orthorhombic cell (solid lines) corresponds to the highest-symmetry magnetic space group ($Cm'c2'$) consistent with the data. The solid circles correspond to Ni ions on the A sites, while the crosses correspond to the Ni, B sites (see text).

VII in Fig. 2) in which the moments on site A are fully disordered, while those on sites B are equal and opposite and are inclined at an angle θ to the c axis. It can easily be shown that the structure factors for this model are identical to those of model VI for $\mu \sim 1.5\mu_B$ and $\theta \sim 42^\circ$. The highest-symmetry magnetic space group consistent with this structure is monoclinic $C2'/c$, with the moments confined to the xz plane.

Although the fit to the data obtained with these two models is identical, model VI is clearly to be preferred. Not only is the symmetry of model

TABLE III. Parameter values obtained from least-squares refinements of the magnetic intensity data from RbNiCl_3 at 4.5°K , for the various models illustrated in Figs. 1 and 2. A more complete description of models I-V can be found in Paper I. $R_w = |\sum W(I_{\text{obs}} - I_{\text{calc}})^2 / \sum W(I_{\text{obs}})^2|^{1/2}$. κ is a scaling factor applied to the form factor and μ is the Ni moment. Standard errors are given in parentheses and refer to the least significant digit(s).

Model	Orientation	μ (μ_B)	κ	R_w
I	(001)	1.02(6)	0.88(8)	0.347
IIa(multidomain)	\perp (001)	1.18(2)	0.83(3)	0.071
IIb(single domain)	\perp (001) ^a	1.13(2)	0.83(1)	0.057
III	[001]	1.96(20)	1.03(15)	0.443
IVa(multidomain)	\perp [001]	1.44(8)	0.88(8)	0.346
IVb(single domain)	\perp [001] ^b	1.30(4)	0.84(4)	0.175
VI(multidomain)	\perp (001)	1.25(2)	0.83(1)	0.057
VII(multidomain)	\perp (001)	1.46(2)	0.83(1)	0.057

^aNormal to spin plane at 23° to [110].

^bSpin direction to 90° to [110].

VI higher than that of model VII, but more important, a straightforward physical mechanism involving competition between exchange interaction and anisotropy exists. For model VII the moments presumably lie along the easy direction of magnetization, but it is difficult to understand why this should not coincide with one of the symmetry axes of the crystal. In isostructural CsCoBr_3 , for example, at 20°K a structure of this sort is indeed observed⁷ but in this case θ is zero within experimental error.

The angle θ for model VI can be derived from the Hamiltonian

$$\mathcal{H} = -\sum_i [2JS_i S_{i+1} + D(S_i^z)^2] \quad (1)$$

For the three atoms in one layer in the unit cell, considering only nearest-neighbor interactions in the basal plane, we have

$$\mathcal{H} = -2JS^2[6\cos(180-\theta) + 3\cos 2\theta] - DS^2(1 + 2\cos^2\theta), \quad (2)$$

$$\frac{\partial \mathcal{H}}{\partial \theta} = -2JS^2(6\sin\theta - 12\sin\theta\cos\theta) + DS^2(4\cos\theta\sin\theta) = 0; \quad (3)$$

$\sin\theta = 0$ minimizes the expression for basal-plane ferromagnetic exchange. For antiferromagnetic exchange we have

$$\cos\theta = +[3J/(6J+D)]. \quad (4)$$

Using Achiwa's values of D and J^1 , we get $\theta \approx 58^\circ$.

The results for the various models considered are summarized in Table III and the observed and calculated magnetic intensities for the triangular

TABLE IV. Comparison of observed and calculated magnetic intensities for the multidomain triangular structure (model IIa) and the modified structure (model VI). I_{obs} is the observed intensity corrected for absorption, and I_{calc} is the calculated intensity based upon the parameters in Tables I and III. The results for model VI apply also to models IIb and VII.

hkl	I_{obs}	I_{calc} (model IIa)	I_{calc} (model VI)
$\frac{1}{3}\frac{1}{3}1$	375.5	395.1	383.3
$\frac{2}{3}\frac{2}{3}1$	351.6	318.8	323.8
111	0.0	0.0	0.0
$\frac{4}{3}\frac{4}{3}1$	157.4	159.5	167.0
$\frac{5}{3}\frac{5}{3}1$	115.1	108.4	114.1
$\frac{7}{3}\frac{7}{3}1$	50.7	47.7	50.4
$\frac{1}{3}\frac{1}{3}3$	65.8	73.5	68.5
$\frac{2}{3}\frac{2}{3}3$	64.9	68.2	64.7
$\frac{4}{3}\frac{4}{3}3$	52.3	49.6	49.0
$\frac{5}{3}\frac{5}{3}3$	44.1	39.0	39.1
$\frac{1}{3}\frac{1}{3}5$	12.1	15.6	14.4

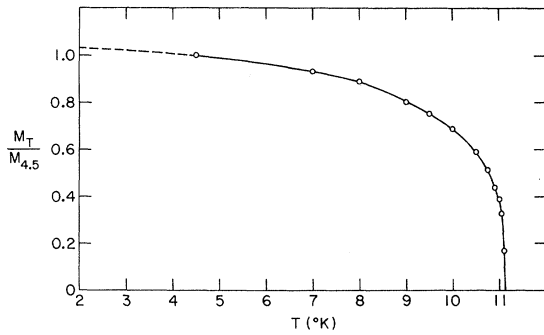


FIG. 4. Magnetization of RbNiCl₃ determined from the intensity of the $(\frac{1}{3}\frac{1}{3}1)$ reflection. Extrapolation to 0°K yields a nickel moment of $1.3\mu_B$.

model IIa and for model VII are compared in Table IV.

III. TEMPERATURE DEPENDENCE OF MAGNETIC MOMENT

The larger crystal was remounted to give an (hhl) zone, and the intensities of the $(\frac{1}{3}\frac{1}{3}1)$ and $(\frac{2}{3}\frac{2}{3}1)$ reflections were studied as a function of temperature, the latter reflection serving as a check for the absence of significant extinction effects. It was very difficult to get accurate data close to T_N because in addition to the low-saturation Ni moment and the sizable nuclear incoherent scattering, there is a high background arising from the one-dimensional ordering which occurs well above T_N . The three-dimensional critical scattering also becomes significant when $\epsilon = [(T_N - T)/T_N]$ is 0.005 or less.

The data close to T_N were corrected for critical scattering as far as possible, and the resulting sublattice magnetization $m \propto (I_{\text{corr}})^{1/2}$ is plotted in Fig. 4. The corrected data can be fitted [Fig. 5(a)] reasonably well between 8.0 and 11.1°K to the power-law expression $I_T/I_{4.5} = A[(T_N - T)/T_N]^{2\beta}$ with $\beta = 0.25 \pm 0.005$, $T_N = (11.105 \pm 0.01)^\circ\text{K}$, and $A = 1.50 \pm 0.02$ (relative errors). T_N agrees well with the value deduced from the maximum in the critical scattering at $(11.15 \pm 0.05)^\circ\text{K}$. The value obtained for β is very close to the values measured for CsNiCl₃⁵ and CsMnBr₃⁷ over similar intervals in reduced temperature, but is distinctly lower than the three-dimensional Ising value, $\beta = 0.31$.⁸ It is, however, much higher than the value of 0.14 ± 0.01 observed in the two-dimensional antiferromagnet K₂NiF₄.⁹

Because of the lack of accurate data close to T_N , a number of points with reduced temperature ϵ between 0.1 and 0.3 have been included in the above derivation, although this is a range over which deviations from the power law are frequently

observed. Therefore, an attempt was made to refit the data to the expression $I_T/I_{4.5} = A[(T_N - T)/T_N]^{2\beta} [1 + C(T_N - T)/T_N]$, which represents a first-order correction to the normal power law.¹⁰ An additional point at 7°K was included, to help define C more accurately, and a better fit was obtained (especially for the range $\epsilon < 0.05$) with $\beta = 0.30 \pm 0.01$, $T_N = (11.15 \pm 0.01)^\circ\text{K}$, $A = 1.95 \pm 0.02$, and $C = -0.45 \pm 0.04$ (relative errors). As shown in Fig. 5(b), this expression in fact gives a satisfactory fit all the way to 4.5°K, the lowest temperature studied. Absolute errors are estimated to be about 0.02, 0.02°K, 0.1, and 0.1, respectively. This value of β suggests critical behavior that is essentially three dimensional and emphasizes the fact that the determination of β from a limited set of data is not necessarily straightforward. It should be noted, however, that for both CsMnCl₃·2H₂O,¹¹ a related "one-dimensional" system which also shows significant one-dimensional correlations well above T_N , and FeCl₂,¹² a system which is predominantly two-dimensional at low temperatures, M_T has been measured over a wider range of ϵ and β has been observed to be very close to 0.30.

The value of the Ni²⁺ moment extrapolated to 0°K is $(1.3 \pm 0.1)\mu_B$ which, as in CsNiCl₃, is surprisingly low. In the approximately octahedral crystal field of the chlorines, the Ni²⁺ moment is typically 2.0–2.2 μ_B . There is no reason, in this case, to attribute the reduced moment to crystal field effects. The low moment can presumably be attributed to the one-dimensional aspects of the system which permit a significant degree of disorder, *in the basal planes*, even at 0°K. Thus it appears that the hexagonal double halides of this type

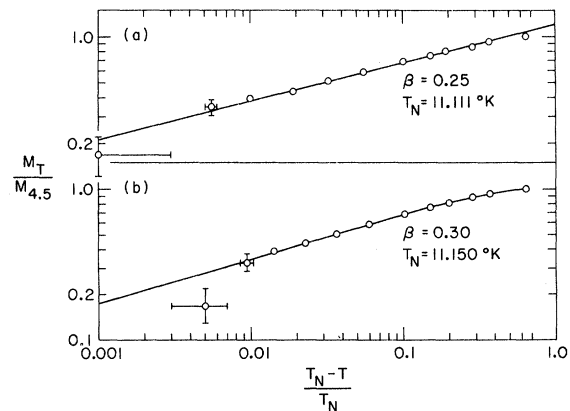


FIG. 5. Fits of the magnetization-vs-temperature data to power-law-type expressions. (a) Simple power law, fitted in the region 8–11°K yielding $\beta = 0.25$. (b) Modified power law (see text) fitted in the region 7–11°K yielding $\beta = 0.30$.

offer a particularly good opportunity to study a rather unusual combination of critical magnetic properties. Further work along these lines is now in progress on CsCoBr_3 and CsMnBr_3 .

ACKNOWLEDGMENT

The authors would like to acknowledge many helpful discussions with J. Sivardière.

[†]Work performed under the auspices of the U. S. Atomic Energy Commission.

¹N. Achiwa, *J. Phys. Soc. Japan* **27**, 561 (1969).

²V. J. Minkiewicz, D. E. Cox, and G. Shirane, *J. Phys. (Paris)* **C1**, 892 (1971).

³V. J. Minkiewicz, D. E. Cox, and G. Shirane, *Solid State Commun.* **8**, 1001 (1970).

⁴A. Epstein, J. Makovsky, and H. Shaked, *Solid State Commun.* **9**, 249 (1971).

⁵D. E. Cox and V. J. Minkiewicz, *Phys. Rev. B* **4**, 2209 (1971).

⁶D. E. Cox and F. C. Merkert, *J. Crystal Growth* (to be published).

⁷W. B. Yelon, D. E. Cox, and V. J. Minkiewicz (unpublished).

⁸D. E. Cox and A. Gottlieb (private communication).

⁹See, for example, G. A. Baker and D. S. Gaunt,

Phys. Rev. **155**, 545 (1967).

¹⁰R. J. Birgeneau, H. J. Guggenheim, and G. Shirane, *Phys. Rev. B* **1**, 2211 (1970).

¹¹This expansion is rigorously correct for the two-dimensional Ising model, and examination of Padé series for different three-dimensional Ising models indicates it is also applicable in those cases [P. J. Kortman and W. B. Yelon (private communication)]. This approach has been tried in the past [J. C. Norvell, W. P. Wolf, L. M. Corliss, J. M. Hastings, and R. Nathans, *Phys. Rev.* **186**, 557 (1969)], but will not produce useful results unless the data extend sufficiently far from T_N for the coefficient C to be well determined.

¹²J. Skalyo, Jr., G. Shirane, S. A. Friedberg, and H. Kobayashi, *Phys. Rev. B* **2**, 1310 (1970).

¹³W. B. Yelon and R. J. Birgeneau, *Phys. Rev. B* **5**, 2615 (1972).

Transition-Temperature Dependences for Diluted Magnetic Systems

John F. Devlin

Solid State Physics Laboratory, University of Groningen, The Netherlands

and

G. A. Sawatzky

Physical Chemistry Laboratory, University of Groningen, The Netherlands

(Received 28 December 1971)

Diluted ferromagnetic and antiferromagnetic Heisenberg systems have been studied by means of three different cluster techniques. The results of two of these methods closely resemble the molecular-field-theory results. The third technique, the usual Bethe-Peierls-Weiss approximation, is shown to have a strong-spin-size-dependent critical concentration for ferromagnetic coupling in contradiction to a rigorous theorem by Rushbrooke and Morgan, while for the antiferromagnetic case no critical concentration exists at zero temperature.

I. INTRODUCTION

Diluted Heisenberg systems have been extensively discussed in the literature (see, for example, Refs. 1-11). The interest in these systems has focused mainly on the dependence of the magnetic transition temperature T_c on the concentration q of nonmagnetic atoms. The most important aspects of a T_c vs q curve are: (a) the slope of the curve near $q=0$, i. e., how T_c changes with small amounts of diluents and (b) the critical concentration q_c above which the system is no longer magnetically ordered even at $T=0$. We are particularly interested here in how the following effect items (a) and (b): the spin size S , the sign of the exchange integral, and

the coordination number z of the lattice. To study these effects we have employed three different cluster techniques.

The usual Bethe-Peierls-Weiss¹² (BPW) cluster technique was first extended by Smart¹ to diluted systems with classical spin vectors associated with each of the magnetic atoms. We repeat here his calculation and in addition include the $S=\frac{1}{2}$ case for both ferromagnetic (FM) and antiferromagnetic (AF) systems. In addition to the BPW choice for the effective fields acting within the clusters we consider two other possible choices which are obtained from a minimization of an approximate free energy. These two choices bear the names of Radcliff¹³ and Hemmann and Brown¹⁴ (HB). The